PAPER *Special Section on Intelligent Signal and Image Processing*

# Unsupervised Optimization of Nonlinear Image Processing Filters Using Morphological Opening/Closing Spectrum and Genetic Algorithm

Akira ASANO†, *Member*

**SUMMARY** It is proposed a novel method that optimizes nonlinear filters by unsupervised learning using a novel definition of morphological pattern spectrum, called "morphological opening/closing spectrum (MOCS)." The MOCS can separate smaller portions of image objects from approximate shapes even if the shapes are degraded by noisy pixels. Our optimization method analogizes the linear low-pass filtering and Fourier spectrum: filter parameters are adjusted to reduce the portions of smaller sizes in MOCS, since they are regarded as the contributions of noises like high-frequency components. This method has an advantage that it uses only target noisy images and requires no example of ideal outputs. Experimental results of applications of this method to optimization of morphological open-closing filter for binary images are presented.

***key words:*** *mathematical morphology, pattern spectrum, nonlinear filter, filter optimization, learning, genetic algorithm*

## 1. Introduction

The nonlinear filters have attracted much attention in the field of image processing, since they have been found to remove nonlinear corruptions on images while preserving image details. However, because of their nonlinearity, it is still difficult to optimally design the nonlinear filters, i.e. to find optimal parameters of the filter in each situation. Recently, the optimization methods by supervised learning have been developed [1]-[5] in which the filter parameters are adjusted by some iterative procedures to reduce the error between the output of an example noisy image and its ideal output. However, the effectiveness of the optimized filter by these methods is not guaranteed for images other than the examples used for the optimization.

The linear filters are optimized without such learning procedures under general criteria based on the Fourier spectrum. In this method, the filter is adjusted to get a desired spectrum in the frequency domain. For example, the noise suppressing filter is optimized to pass components of lower frequency and suppress higher ones. If there exists the nonlinear counterpart of the Fourier spectrum, some nonlinear filters can be designed not by learning procedures using example images but by a general method that is independent on the examples. The pattern spectrum (PS) [6] seems to be a counterpart based on the mathematical morphology [7], [8], which is a general class of the shift-invariant nonlinear image transformation. Like the Fourier transformation decomposes an image to the contributions to the spatial frequencies, PS decomposes an image to the contributions to "sizes." Here the size is defined as how large area an image object occupies in the view of an image. In other words, PS expresses how large and how many objects are needed to decompose an image to an object of basic shape and similar figures of this object. The morphological spectra, as well as PS or size distribution, have been recently popularly investigated [9]-[13].

The morphological filter family, including the rank-order filters, removes impulsive noises quite efficiently, since it removes objects of small sizes by regarding them as noises regardless of the pixel values. Examining spectrum of an image from the size's point of view seem to be useful to analyze and design such filters. From the analogy between the Fourier spectrum and PS, it is natural to reach an idea to apply PS to the optimization of the morphological filters. In case of noise removal, the filter should be supposed to be optimized to suppress portion of smaller sizes on PS, since the portion of smaller sizes may be considered as the contributions of noises.

However, this approach using the conventional PS is not possible to realize for the following reason. The conventional PS is based on opening, which is one of the basic operations of the mathematical morphology and which removes portions smaller than a structuring element (SE), an object of a basic shape. The spectral value of PS for size $n$ with an SE is defined as the area which is preserved by the opening by the SE of size $n$ but eliminated by the opening by the SE of size $n$+1. Here the SE of size $n$ is defined as the $n$-times magnified image of the SE of size 1. Since the opening never fills up any area of the background, the image opened by the SE of size $n$+1 is always included by that opened by the SE of size $n$ (this property is called antiextensivity [14] ). Now suppose a white square on the black background and the same square with one pixel replaced by black one, as shown in Figs. 1(a) and (b). The black spot in the latter square is preserved during the process to calculate the conventional PS with a square SE because of the antiextensivity of the opening, as shown in Figs. 1(c) and (d). In these figures, the horizontal axis indicates the size and the vertical one indicates the contribution (i.e. area or number of pixels) to each size. The information that the latter square can approximately be regarded as one large

Manuscript received May 14, 1999.
Manuscript revised August 19, 1999.

† The author is with the Division of Mathematical and Information Sciences, Faculty of Integrated Arts and Sciences, Hiroshima University, Higashi-Hiroshima-shi, 739-8521 Japan.

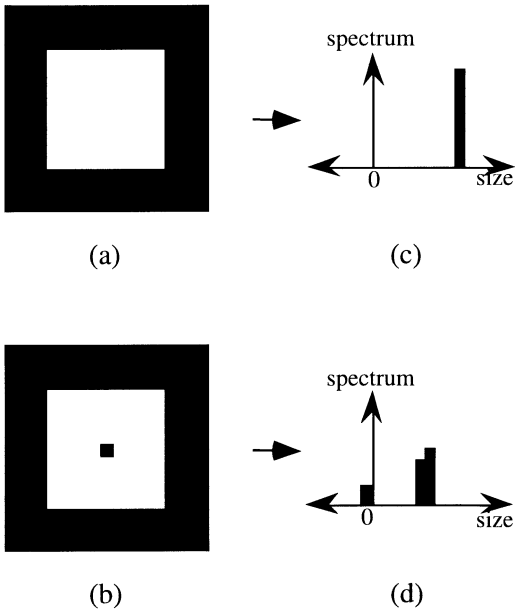


**Fig. 1** A defect of the conventional PS. (a) spectrum for a complete square (white on black background). (b) spectrum for a square with a spot of one pixel. The peak for the large spot vanishes, and the spectrum is quite different from (a).

square is never extracted by the conventional PS. This suggests that a small modification on an image (the replacement of a white pixel with a black one in this case) causes a quite different spectrum, and the information about approximate views of the image is never extracted by the conventional PS. Consequently, the conventional PS could not separate the contributions of noises from the original figure. The design of linear filters using the Fourier spectrum determines the parameters such as cutoff frequencies in accordance with the idea that the contributions of signals and noises are separated on the axis of the frequency. The design of the morphological filter family in the same way using the conventional PS is, however, impossible because the conventional PS cannot separate small black areas, regarded as noisy pixels, from larger figures.

We recently proposed a new concept called "morphological opening/closing spectrum (MOCS)" † [15], [16] to separate noises from larger figures. The MOCS introduces the morphological closing process to the conventional PS. When the contribution to a size is calculated on the process of MOCS, black areas smaller than the size have already been filled up by the closing operations. Thus MOCS can extract the approximate views of large figures while avoiding the influence of small black areas in the figure. Consequently, MOCS can separate the area of noisy pixels from the large meaningful figures; thus MOCS is applicable to the filter optimization method based on the concept that the smaller-size portions on MOCS should be suppressed by the noise removal, like the higher components in the Fourier spectrum.

In this paper, we propose a novel optimization method of nonlinear filters by unsupervised learning using MOCS. The basic scheme of our method is an iterative procedure: a filter with a set of parameters is applied to a target noisy image to calculate MOCS of the filter output. Then the parameter is modified so that the modified filter is applied to the target image again for the MOCS calculation. If the smaller portion of the latter MOCS is suppressed better than that of the former, this modification should be accepted. In our method, these are iterated until the optimized filter is obtained. We apply the genetic algorithm [17], [18] to the method since it performs the procedure quite effectively. Our method realizes the optimization of the filter using only the target noisy image, and not using any example of ideal images.

This method is applicable to optimization of any filters, including non-morphological filters, since the procedures of this method are not related to any typical filtering algorithm. It can also be applied to the optimization of the weighted median filter by modifying the weighted coefficients following to the spectral values of MOCS. In this paper we apply our method to the optimization of morphological open-closing filters for binary images, because of the limitation of computational efficiency. We restrict ourselves to the case of binary images in the following of this paper.

In Sect. 2, we give a brief introduction to the mathematical morphological operations and explain the concept of PS and MOCS. Our novel optimization method using MOCS and the genetic algorithm is explained in Sect. 3. The experimental results of optimization of morphological filters for binary images are shown in Sect. 4. Finally we conclude this work in Sect. 5.

## 2. Morphological Opening / Closing Spectrum (MOCS)

### 2.1 Mathematical Morphological Operations

We first show some basic and important morphological operations. We assume binary images for discussions in this paper. Images are regarded as sets whose elements are the coordinates of the pixels contained by the objects in the image. Here a structuring element is introduced: this is also a set of coordinates and is compared to the window of image processing filters. The most basic morphological operations, erosion and dilation, of image $X$ by the structuring element $B$ are defined as follows:

$$\begin{cases} \text{erosion: } X \ominus \check{B}, \\ \text{dilation: } X \oplus \check{B}, \end{cases} \tag{1}$$

where $\check{B}$ denotes the inversion of $B$ against the origin, defined as follows:

† In Refs. [15], [16], this method is referred as "multiresolution pattern spectrum." It has been renamed since the term "multiresolution" is confusing as if this method were related to the multiresolution analysis using the wavelet transform.

$$\check{B} = \{-\boldsymbol{b} \mid \boldsymbol{b} \in B\}, \tag{2}$$

and, $\ominus$ and $\oplus$ are called the Minkowski set subtraction and addition, respectively, defined as follows:

$$\begin{cases} X \ominus B = \bigcap_{\boldsymbol{b} \in B} X_{\boldsymbol{b}}, \\ X \oplus B = \bigcup_{\boldsymbol{b} \in B} X_{\boldsymbol{b}}, \end{cases} \tag{3}$$

where $X_{\boldsymbol{b}}$ denotes the translation of $X$ by the vector $\boldsymbol{b}$, defined as follows:

$$X_{\boldsymbol{b}} = \{\boldsymbol{x}+\boldsymbol{b} \mid \boldsymbol{x} \in X\}. \tag{4}$$

Applied to an image, the erosion shrinks the objects and eliminates fragments smaller than the SE, and the dilation expands the objects by the size of the SE and fills up black spots smaller than the SE. Here the term "smaller than the SE" means "completely included by the SE."

Opening and closing are the combinations of the erosion and dilation, and are the most important basic operations, defined as follows:

$$\begin{cases} \text{opening: } X_B = \left(X \ominus \check{B}\right) \oplus B \\ \text{closing: } X^B = \left(X \oplus \check{B}\right) \ominus B \end{cases}. \tag{5}$$

Figure 2 illustrates the effect of these four operations. The opening shrinks the objects and eliminates the portion of the objects smaller than the SE by the erosion, and then the following dilation restores the shrunk objects. The portion larger than the SE is not completely eliminated by the preceding erosion and then restored by the following dilation. However, the portion smaller than the SE is completely eliminated by the erosion and never restored by the dilation. Thus, the opening eliminates the portion smaller than the SE while preserving the other portion of the objects. The closing is the complement: it fills up smaller spots while preserving the other portion of the background. This ability of the opening and closing to quantify the size distribution of objects is important for defining PS and MOCS.

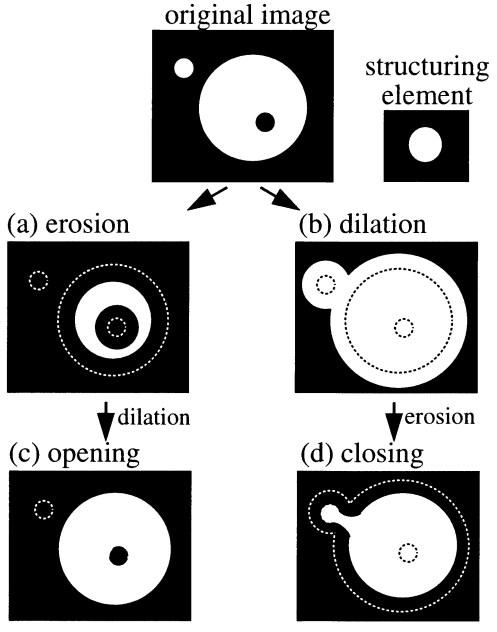


**Fig. 2** Basic morphological operations. (a) erosion, (b) dilation, (c) opening, and (d) closing.

## 2.2 Pattern Spectrum and Morphological Opening/Closing Spectrum

The pattern spectrum (PS) of size $n$ by an SE is defined as the area of white pixels which are contained by an image opened by the similarly magnified sets of SE of size $n$ but not contained by the image opened by SE of size $n$+1. Let $nB$ be the similar magnification of a structuring element $B$ of size $n$, defined as follows:

$$\begin{aligned} &nB = \underbrace{B \oplus B \oplus \ldots \oplus B}_{n-1 \text{ times}} \quad n>0, \\ &0B = \{\boldsymbol{0}\}. \end{aligned} \tag{6}$$

Then the PS of size $n$ by the structuring element $B$ for image $X$, denoted as PS($X$, $B$, $n$), is defined as follows:

$$\mathrm{PS}(X, B, n) = A\left(X_{nB} - X_{(n+1)B}\right) \tag{7}$$

where $A(Y)$ is the cardinality of the set $Y$ (i.e. the area of objects in $Y$, or the number of white pixels in the image $Y$), and $X$–$Y$ denotes the set difference, defined as follows:

$$X - Y = \{a \mid a \in X \text{ and } a \notin Y\}. \tag{8}$$

Since the opening operation removes the portion smaller than the SE, the difference of the images opened by the SEs of size $n$ and size $n$+1 contains the portion whose size is exactly $n$.

The morphological opening/closing spectrum (MOCS) is defined by introducing the closing processes into the definition of the conventional pattern spectrum. The MOCS of size 0 by the structuring element $B$ is defined as follows:

$$\mathrm{MOCS}(X, B, 0) = A\left(X - X_B\right) \tag{9}$$

i.e. the same as PS($X$, $B$, 0). The MOCS of size $n$>0 is defined as follows:

$$\mathrm{MOCS}(X, B, n) = A\left(\left(\mathrm{OC}(X, B, n)\right)_{nB} - \left(\mathrm{OC}(X, B, n)\right)_{(n+1)B}\right) \tag{10}$$

where OC($X$, $B$, $n$) is defined recursively as follows:

$$\begin{aligned} &\mathrm{OC}(X, B, n) = \left(\left(\mathrm{OC}(X, B, n-1)\right)_{(n-1)B}\right)^{nB} \quad n>1, \\ &\mathrm{OC}(X, B, 1) = X^B, \\ &\mathrm{OC}(X, B, 0) = X. \end{aligned} \tag{11}$$

PS and MOCS of $n \le 0$ are defined by interchanging opening and closing in the above definitions for size $|n|$. This

means that MOCS for positive sizes and MOCS for negative sizes are dual operations: MOCS for negative sizes extracts black objects in the white background. Note that there are two definitions for size $n$=0: one using the definition for $n \geq 0$ is denoted as MOCS($X$, $B$, +0) and the other, using the definition for $n \leq 0$, is denoted as MOCS($X$, $B$, –0). These two are different: MOCS($X$, $B$, +0) is the area eliminated by the opening of size 1, and MOCS($X$, $B$, –0) is the area filled by the closing of size 1.

When MOCS of size $n \geq 0$ is calculated, a black spot smaller than size $n$ within an object has already been filled up by the closing operation of size $n$, and no longer exists in the image OC($X$, $B$, $n$). Thus, the portion of size $n$ is extracted by the opening operations without any influences of noisy spots smaller than $n$. This idea is similar to the concept of alternative sequential filter (ASF). A novel image pyramid based on ASF has been investigated [19]. Note that MOCS is obviously not anti-extensive.

We show examples of PS and MOCS for some typical figures. In this example SE of size 1 is 3×3-pixel square and spectra for only positive sizes are calculated. Figure 3(a) shows a complete square of 13×13 pixels. The spectra by PS and MOCS are the same in this case, as shown in Table 1(a): a peak appears at size 6. Figure 3(b) shows the square with a spot of one pixel and the spectra are shown in Table 1(b). In PS peaks appear only at size 2 and 3, and the peak at size 6 does not appear. On the other hand, MOCS still extracts the peak for whole square. The influence of the spot in the square appears in spectral values of MOCS for negative sizes. Figure 3(c) shows the square with a spot of 3×3 pixels, and the spectra are shown in Table 1(c). In this case, the MOCS extracts the narrow part above the spot in the square as well as the whole square, since the size of this part is as small as the size of the spot.

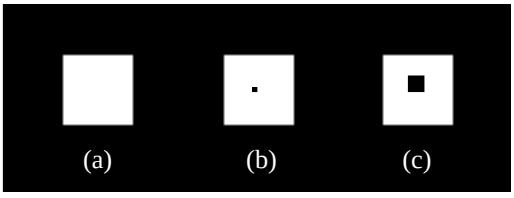


**Fig. 3** Examples of typical figures. (a) square of 13×13 pixels. (b) square with one-pixel spot. (c) square with 3×3-pixel spot.

**Table 1** Spectral values of Fig. 3 by PS and MOCS for positive sizes.

(a) complete square

| size | +0 | +1 | +2 | +3 | +4 | +5 | +6 | +7 |
|---|---|---|---|---|---|---|---|---|
| PS | 0 | 0 | 0 | 0 | 0 | 0 | 169 | 0 |
| MOCS | 0 | 0 | 0 | 0 | 0 | 0 | 169 | 0 |

(b) square with a spot of one pixel

| size | +0 | +1 | +2 | +3 | +4 | +5 | +6 | +7 |
|---|---|---|---|---|---|---|---|---|
| PS | 0 | 0 | 77 | 91 | 0 | 0 | 0 | 0 |
| MOCS | 0 | 0 | 0 | 0 | 0 | 0 | 169 | 0 |

(c) square with a spot of 3×3 pixels

| size | +0 | +1 | +2 | +3 | +4 | +5 | +6 | +7 |
|---|---|---|---|---|---|---|---|---|
| PS | 0 | 12 | 148 | 0 | 0 | 0 | 0 | 0 |
| MOCS | 0 | 12 | 0 | 0 | 0 | 0 | 169 | 0 |

## 3. Unsupervised Filter Optimization Using MOCS and Genetic Algorithm

### 3.1 Strategy of Optimization

The strategy of the unsupervised optimization by MOCS is reducing the spectral values of MOCS of the target noisy image for small sizes since these are regarded as the contributions of noises, and preserving the values for larger sizes since these are regarded as the contributions of meaningful figures. The method is schematically illustrated in Fig. 4. Suppose that the MOCS of target noisy image is such distribution as shown in Fig. 4(a), where the axes are similar to Figs. 1(c) and (d). We generate a distribution as shown in Fig. 4(b). This is similar to the distribution in Fig. 4(a) but spectral portions of small sizes are suppressed. This distribution is considered as the spectrum of ideally filtered image. An initial filter with a certain set of parameters is generated first, and then it is applied to the noisy image. The optimization process calculates the error between the MOCS of the output by the initial filter (Fig. 4(c)) and the ideal MOCS shown in Fig. 4(b). Then the filter optimization process modifies the parameters of the filter to reduce the error and finally obtains the ideal set of parameters.

The filter optimization process iterates the above two procedures — the evaluation of the error and the

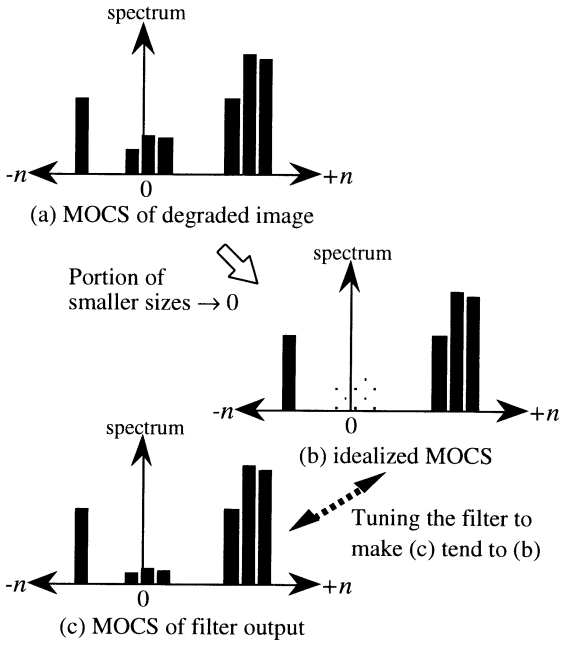


**Fig. 4** Concept of filter optimization using MOCS.

modification of the filter parameters — until the error is reduced sufficiently small. To realize this process, we require a method that modifies the parameters randomly and slightly, and that chooses the modifications leading the error to the minimum. The simulated annealing and the genetic algorithm are available techniques for this purpose. We apply the genetic algorithm and describe in the next subsection how we adopt it to our method.

It is a problem what structuring elements should be used for the evaluation of MOCS. If the objective of the filter design is to preserve a specific shape, the structuring element of this shape should be chosen. In general cases, it is better to calculate MOCSs with the structuring elements of several typical shapes and evaluate the summation of errors for each structuring element.

### 3.2 Adaptation of Genetic Algorithm

In this paper we apply the genetic algorithm to our optimization algorithm. Application of the genetic algorithm to the filter optimization has been already reported [17]. The method in [17] is based on supervised learning that requires an example of ideal output of the target filter. Our method is, however, unsupervised learning method that requires no example of ideal output. We explain in this subsection how the genetic algorithm is adopted.

*Step 1. Encoding filter parameters to genes*
The genetic algorithm encodes one parameter set to an individual which has one or several genes. Each gene is a sequence of 0 / 1 - bits and is assigned for one filter window or structuring element. In case of our experiment described in the next chapter, since we optimize the SE-shapes of the morphological filter, we assign 1 if the pixel at a relative position from the origin of the SE constitutes in the SE, and assign 0 otherwise, as shown in Fig. 5(a). When the filter has several SEs, an individual has several genes as shown in Fig. 5(b).

*Step 2. Initial evaluation of genes*
We initially generate a set of individuals. The number of individuals is denoted as $P_{num}$. Then we evaluate each individual by MOCS. Formally explaining, we calculate the error function $E(X, B, I)$ by the following:

$$E(X,B,I) = \sum_{n=-N_{max}}^{N_{max}} W_n\left\{\mathrm{MOCS}_I(X,B,n) - \mathrm{MOCS}_{id(N_{noise})}(X,B,n)\right\}, \tag{12}$$

where $N_{max}$ is the maximum size at which MOCS is calculated, $\mathrm{MOCS}_I(X, B, n)$ is the spectral value of size $n$ using the SE $B$ for the target image $X$ filtered by the individual $I$, and $W_n$ is the weight for each $n$. $\mathrm{MOCS}_{id(N_{noise})}$ is the identical MOCS, denoted as follows:

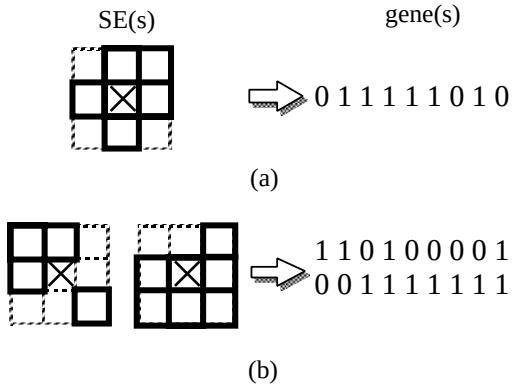


**Fig. 5** Configuration of a gene. The symbol × in each SE indicates the origin, and squares surrounded by thick lines indicate pixels contained by SEs. (a) In the case where the filter has only one SE. (b) In the case where the filter has two SEs.

$$\mathrm{MOCS}_{id(N_{noise})}(X,B,n) = \begin{cases} 0 & \text{if } -N_{noise} \le n \le N_{noise}, \\ \mathrm{MOCS}(X,B,n) & \text{otherwise,} \end{cases} \tag{13}$$

where $\mathrm{MOCS}(X, B, n)$ is the spectral value of size $n$ using the SE $B$ for the target image $X$ itself, as defined in Sect. 2, and $N_{noise}$ is the parameter determining how small-size portion should be regarded as noisy pixels.

*Step 3. Modifications of genes*
The individuals are modified by genetic operations. In our method, "selection," "crossover," and "mutation" are applied in this order.
i) Selection — This "selection" operation makes a sequence of the individuals in order of increasing error. Then it selects a certain number of high-ranking individuals from the sequence. The residual individuals are eliminated. The ratio of the number of selected individuals to $P_{num}$ is denoted as $S_{rate}$.
ii) Crossover — The "crossover" reproduces a new individual whose genes are created by a mixture of those existing in the two individuals called "parents," which are chosen randomly from the individuals selected in the previous step. We apply the method of uniform crossover. As shown in Fig. 6, the value at each position of the new gene is chosen from the value at the corresponding position of either of two parents at an equal probability. In this stage $P_{num}(1–S_{rate})$ individuals are generated to compensate those eliminated in the previous step.
iii) Mutation — The "mutation" flips some bits of a gene randomly at a certain probability. We apply the mutation only to the individuals which are compensated in the previous step. The probability of flipping each bit is denoted as $M_{rate}$.

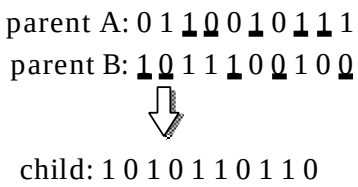


**Fig. 6** Uniform crossover. The child is produced by combining randomly selected elements of the parents (underlined ones).

*Step 4. Final evaluation*

Each individual compensated in the previous step is evaluated by the same procedure as the step 2. If smallest error produced by the individuals of the set is sufficiently small, we treat this individual as the result of our method. Otherwise, step 3 is applied again for the evaluation. In our experiment, these steps are repeated certain times, denoted by $G_{max}$, and finally the smallest error of the individuals is chosen as the result of our method, for simplicity.

## 4. Experimental Results

We optimize the binary morphological open-closing (OC) filter [20] with three SEs of 3×3 pixels. The OC filter applies the opening by each SE independently to the target image, generates an temporary image by pixelwise OR of the opened images, applies the closing by the same SEs to the temporary image, and then generates the final output by pixelwise AND of the closed images. The optimization algorithm modifies the shape of each SE within the square of 3×3 pixels. In step 2 and 4 of the previous section, we calculate the sum of each errors calculated by Eq. (12) using B as each of six SEs as shown in Fig. 7. Note that these six SEs are not related to the SEs of the OC filters to be optimized: the optimization algorithm is not dependent on the filtering algorithms to be optimized.

Figure 8 demonstrates the effectiveness of our method. Figure 8(a) is the target noisy binary image, which is a symbolic figure of 30×30 pixels and is corrupted by the salt-and-pepper noise of probability 15%. Figure 8(b) shows the output of the OC filter with one full-square SE of 3×3 pixels and no AND or OR operation. This filter is the most effective for noise removal in the class of OC filters with SE of 3×3 pixels. The output shows that this unoptimized OC filter removes noisy pixels effectively but loses details of the object. Figure 8(c) shows the output of the resultant filter by our optimization method. The parameters are the followings: $P_{num} = 50$, $G_{max} = 20$, $S_{rate} = 40$, $M_{rate} = 0.02$, $N_{max} = 8$, $N_{noise} = 1$, $W_0 = 20$, $W_1 = 10$, $W_2 = 5$, and $W_3 = \ldots = W_8 = 1$. The resultant filter by our method yields better output than the unoptimized one. The number shown on each figure indicates the ratio of pixels whose values are different from the pixels of corresponding positions in the original noiseless image, shown in Fig. 8(d). Note that this image is unknown in real cases, and is used only for reference in this experiment.

Another example is shown in Fig. 9. Figure 9(a) shows the target image, which is the character "E" of 30×30 binary pixels and is corrupted by the salt-and-pepper noise of probability 15%. Figure 9(b) shows the output of the OC filter with a full-square SE of 3×3 pixels. Although it removes noisy pixels well, it scrapes many parts off the character and completely cuts the highest beam of the

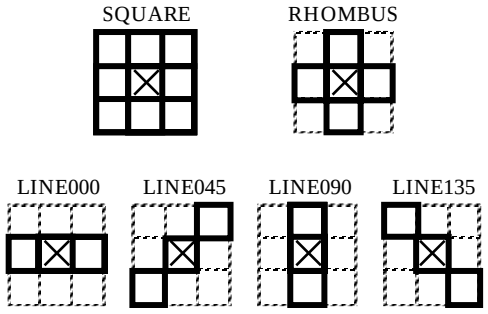


**Fig. 7** Structuring elements used in the optimization process of our experiments. The symbol × and squares surrounded by thick lines are the same as Fig. 5.

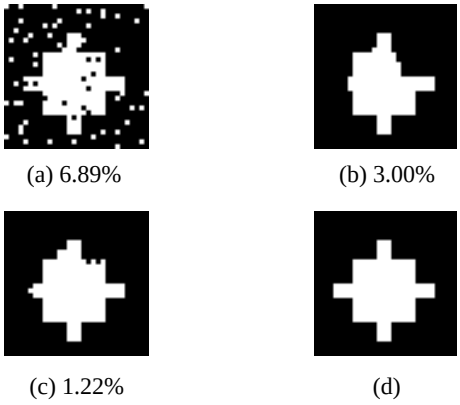


**Fig. 8** Experimental results. (a) target noisy image. (b) output of unoptimized OC filter. (c) output of the OC filter optimized by our method. (d) original noiseless image (for reference). The number on each image indicates the ratio of pixels that are different from the pixel at corresponding position of the reference image (d) .

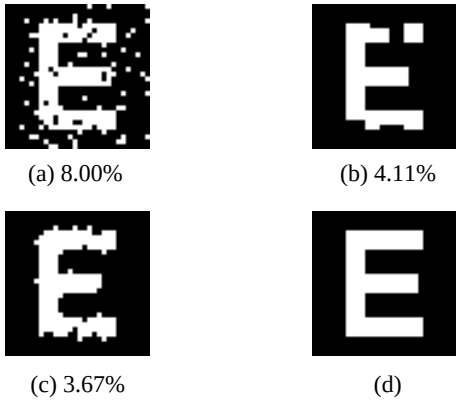


**Fig. 9** Experimental results. (a) target noisy image. (b) output of unoptimized OC filter. (c) output of the OC filter optimized using "LINE000" and "LINE090" only. (d) original noiseless image (for reference). The number on each image is similar to Fig. 8.

**Table 2** Spectral values of Fig. 9(a) by MOCS using SEs in Fig. 7.

| size | +0 | +1 | +2 | +3 | +4 | +5 | +6 | +7 | +8 |
|---|---|---|---|---|---|---|---|---|---|
| SQUARE | 96 | 161 | 0 | 0 | 0 | 0 | 0 | 0 | 0 |
| RHOMBUS | 78 | 14 | 78 | 15 | 50 | 46 | 0 | 136 | 0 |
| LINE000 | 60 | 31 | 5 | 7 | 0 | 0 | 41 | 125 | 35 |
| LINE045 | 72 | 81 | 31 | 67 | 10 | 46 | 13 | 31 | 0 |
| LINE090 | 62 | 97 | 16 | 16 | 0 | 0 | 39 | 32 | 0 |
| LINE135 | 78 | 64 | 35 | 37 | 18 | 33 | 0 | 15 | 0 |

| size | –0 | –1 | –2 | –3 | –4 | –5 | –6 | –7 | –8 |
|---|---|---|---|---|---|---|---|---|---|
| SQUARE | 96 | 9 | 0 | 0 | 0 | 0 | 0 | 0 | 0 |
| RHOMBUS | 42 | 16 | 54 | 0 | 0 | 0 | 0 | 0 | 0 |
| LINE000 | 29 | 0 | 0 | 0 | 0 | 0 | 0 | 0 | 0 |
| LINE045 | 50 | 22 | 0 | 0 | 0 | 0 | 0 | 0 | 0 |
| LINE090 | 40 | 12 | 15 | 0 | 0 | 0 | 0 | 0 | 0 |
| LINE135 | 53 | 15 | 10 | 0 | 0 | 0 | 0 | 0 | 0 |

character “E,” since noisy pixels are concentrated there.

Table 2 shows the spectral values of Fig. 9(a) by MOCS using SEs in Fig. 7. The spectrum by “SQUARE” SE has no peaks at larger sizes. If this spectrum is used for the evaluation processes of the optimization process, the filter is trained to suppress all the spectral values and it may lose details similarly to the unoptimized OC filter with a full-square SE. The spectra by “LINE000” and “LINE090” SEs have obvious peaks at large positive sizes. These peaks are separated well from the portion at small sizes†. This suggests that contribution by noisy pixels and that by original figures are separated well in these spectra. Figure 9(c) shows the output of the OC filter optimized using SEs of “LINE000” and “LINE090” only. Although some noisy pixels remain in the output, the beam cut in Fig. 9(b) is remained connected and ratio of erroneous pixels is smaller. These results show that the optimization method selects a suitable filter under a trade-off between preservation of details and complete noise removal with loss of details by selecting SEs for evaluation of MOCS, under the condition that the target filter is restricted to the class of OC filters with three 3×3-pixel SEs.

## 5. Conclusions

The unsupervised optimization method of nonlinear filters using MOCS and the genetic algorithm has been described in this paper. Our method realizes the optimization of a filter using the target noisy image only, while the conventional supervised learning methods require an example pair of noisy images and their ideal outputs. The experimental results show the effectiveness of the optimized filter by our method for binary images. The MOCS has been proposed as a key to solve the problem “HOW the nonlinear filters work?” which has been pursued for long years. Further theoretical works on this topic should be our future problem. The extension of the MOCS and the optimization method to larger and grayscale images and to other filters will also be interesting works.

† As illustrated in Fig. 3 and Table 1, these peaks in larger sizes (6, 7) obviously do not appear in the spectra of the conventional PS since the black spots within the white “E” are never removed by the calculating process of the conventional PS. This is an example to explain the reason why MOCS instead of the conventional PS should be used for filter optimization.

## Acknowledgments

The author wishes to thank Dr. Alexander Tuzikov, who is a principal researcher of the Institute of Engineering Cybernetics, Beralus Academy of Sciences, for his meaningful comments. The author also wishes to thank Mr. Takahiro Honda, who was a graduate student in our laboratory, for his contribution to the experiments.

### References

[1] A.Asano, K.Itoh, and Y.Ichioka, “Optimization of the weighted median filter by learning,” Opt. Lett., vol.16, pp.168-170, 1991.
[2] A.Asano, K.Itoh, and Y.Ichioka, “Optimization of cascaded threshold logic filters for grayscale image processing,” Opt. Commun., vol.88, pp.485-493, 1992.
[3] A.Asano, K.Matsumura, K.Itoh, Y.Ichioka, and S.Yokozeki, “Optimization of morphological filters by learning,” Opt. Commun., vol.112, pp.265-270, 1994.
[4] A.Asano, T.Yamashita, and S.Yokozeki, “Learning optimization of morphological filters with grayscale structuring elements,” Opt. Eng., vol.35, pp.2203-2213, 1996.
[5] L.Yin, J.Astola, and Y.Neuvo, “A new class of nonlinear filters — Neural filters,” IEEE Trans. Signal Process., vol.41, pp.1202-1222, 1993.
[6] P.Maragos, “Pattern spectrum and multiscale shape representation,” IEEE Trans. Pattern Anal. & Mach. Intell., vol.11, pp.701-716, 1989.
[7] J.Serra, Image Analysis and Mathematical Morphology, Academic Press, London, 1982.
[8] R.M.Haralick, S.R.Sternberg, and X.Zhuang, “Image analysis using mathematical morphology,” IEEE Trans. Pattern Anal. & Mach. Intell., vol.PAMI-9, pp.532-550, 1987.
[9] R.M.Haralick and P.L.Katz, “Model-based morphology: The opening spectrum,” Graphical Models and Image Processing, vol.57, pp.1-12, 1995.
[10] E.R.Dougherty, “Optimal binary morphological bandpass filters induced by granulometric spectral representation,” Journal of Mathematical Imaging and Vision, vol.7, pp.175-192, 1997.
[11] A.Toet, “A morphological pyramidal image decomposition,” Pattern Recognit. Lett., vol.9, pp.255-264, 1989.
[12] A.Morales, R.Acharya, and S.-J.Ko, “Morphological pyramids with alternating sequential filters,” IEEE Trans. Image Process., vol.4, pp.965-977, 1995.
[13] A.Toet, “A hierarchical morphological image decomposition,” Pattern Recognit. Lett., vol.11, pp.267-274 , 1990.
[14] J.Serra, “Introduction to mathematical morphology,” Computer Vision, Graphics, Image Process., vol.35, pp.283-305, 1986.
[15] A.Asano and S.Yokozeki, “Morphological multiresolution pattern spectrum,” IEICE Trans. Fundamentals, vol.E80-A, no. 9, pp.1662-1666, Sept. 1997.
[16] A.Asano and S.Yokozeki, “Multiresolution pattern spectrum and its application to optimization of nonlinear filter,” Proc.

1996 International Conference on Image Processing, Lausanne, Switzerland, pp.387-390, 1996.

[17] N.R.Harvey and S.Marshall, "The use of genetic algorithm in morphological filter design," Signal Processing: Image Communication, vol.8, pp.55-71, 1996.

[18] S.Loncaric and A.P.Dhawan, "Optimal shape description using morphological signature transform via genetic algorithm," Image Algebra and Morphological Image Processing IV, Proc. SPIE, vol.2030, pp.121-127, 1993.

[19] A.Morales, R.Acharya, and S.-J.Ko, "Morphological pyramids with alternating sequential filters," IEEE. Trans. Image Process., vol.4, no.7, pp.965-977, 1995.

[20] R.L.Stevenson and G.R.Arce, "Morphological filters: Statistics and further syntactic properties," IEEE Trans. Circuits & Syst., vol.CAS-34, no.11, pp.1292-1305, 1987.

**Akira Asano** received the B.Eng., M.Eng., and Ph.D. degrees in Applied Physics from Osaka University, Osaka, Japan, in 1987, 1989, and 1992, respectively. From 1992 to 1998, he was a research associate of the Department of Mechanical System Engineering, Kyushu Institute of Technology. Since 1998, he has been an associate professor of the Division of Mathematical and Information Science, Faculty of Integrated Arts and Sciences, Hiroshima University. On September and October in 1990, he was a guest scientist of the Information Transmission Problems, the USSR Academy of Sciences. From May 1994 to February 1995, he was a guest scientist of VTT (Technical Research Centre of Finland) Information Technology. His current research interests are in the area of image processing, especially theoretical researches of frameworks of image expression and the mathematical morphology, and statistical analysis of images. He is a member of the Institute of Image Information and Television Engineers, SPIE, and IEEE. He received the award for excellent poster presentations in the 24th Joint Conference on Imaging Technology (Tokyo, Japan) in 1993.
E-mail: asano@mis.hiroshima-u.ac.jp
WWW: http://www.mis.hiroshima-u.ac.jp/~asano/